

THE DISTRIBUTION OF QUASARS AND GALAXIES IN RADIO COLOR-COLOR AND MORPHOLOGY DIAGRAMS

Ž. IVEZIĆ, R.J. SIVERD, W. STEINHARDT, A.S. JAGODA, G.R. KNAPP,
R.H. LUPTON, D. SCHLEGEL, P.B. HALL, G.T. RICHARDS, J.E. GUNN,
M.A. STRAUSS, M. JURIĆ, AND P. WIITA

*Department of Astrophysical Sciences
Princeton University, Princeton, NJ 08544, USA*

M. GAČEŠA AND V. SMOLČIĆ

*Department of Physics
University of Zagreb, Bijenička Cesta 4, Zagreb, Croatia*

We positionally match the 6 cm GB6, 20 cm FIRST and NVSS, and 92 cm WENSS radio catalogs and find 16,500 matches in $\sim 3,000$ deg² of sky. Using this unified radio database, we construct radio “color-magnitude-morphology” diagrams and find that they display a clear structure, rather than a random scatter. We propose a simple, yet powerful, method for morphological classification of radio sources based on FIRST and NVSS measurements. For a subset of matched sources, we find optical identifications using the SDSS Data Release 1 catalogs, and separate them into quasars and galaxies. Compact radio sources with flat radio spectra are dominated by quasars, while compact sources with steep spectra, and resolved radio sources, contain substantial numbers of both quasars and galaxies.

1. The Era of Modern Radio Surveys

Statistical studies of the radio emission from extragalactic sources are entering a new era due to the availability of large sky area high-resolution radio surveys that are sensitive to mJy levels (e.g. FIRST, Becker, White & Helfand 1995; GB6, Gregory et al. 1996; WENSS, Rengelink et al. 1997; NVSS, Condon et al. 1998). The catalogs based on these surveys contain millions of sources, have high completeness and low contamination, and are available in digital form. The wide wavelength region spanned by these surveys, from 6 cm for GB6 to 92 cm for WENSS, and the detailed morphological information at 20 cm provided by FIRST and NVSS, allow significant quantitative and qualitative advances in studies of radio sources.

Here we present a preliminary analysis of sources detected by the GB6,

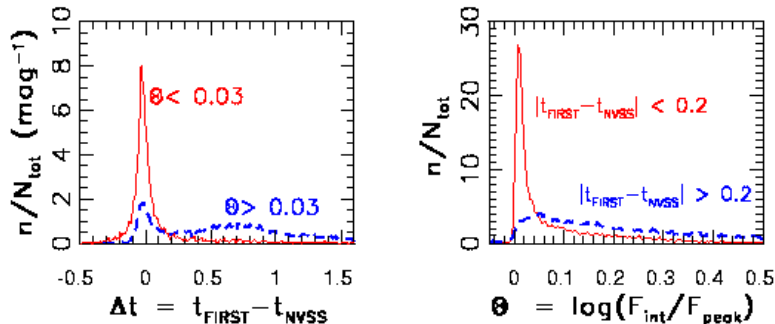


Figure 1. The bimodal distribution of the $\Delta t = t_{FIRST} - t_{NVSS}$ magnitude differences (left). This bimodality essentially reflects the separation between isolated core sources ($|\Delta t| < 0.2$) and lobe and complex sources ($|\Delta t| > 0.2$). We confirmed this conclusion by visually inspecting about 1000 $2' \times 2'$ FIRST images (Ivezić et al. 2004, in prep). The majority of lobe and complex sources, and some core sources, are resolved by FIRST on 5 arcsec scale ($\Theta > 0.03$, right panel).

NVSS, FIRST and WENSS radio surveys, and of the subset also detected by the optical Sloan Digital Sky Survey (SDSS; York et al. 2000; Stoughton et al. 2002, and references therein). Matching FIRST and NVSS allows a robust estimate of the source morphology at 20 cm, and the addition of GB6 and WENSS data allows the determination of the radio spectral slope and curvature. SDSS identifications enable the separation of sources into quasars and galaxies, and, for some objects, also provides the redshifts.

2. The Cross-identification of Radio Sources

The cross-identification of radio surveys at different wavelengths, and with different resolutions, is not straightforward (e.g. Becker et al. 1995; Ivezić et al. 2002). However, the accurate positions provided by FIRST allow simple positional matching with high completeness and a low random contamination rate. Based on an analysis of positional differences, we adopted maximum positional discrepancies between FIRST and the other three surveys of $15''$, $30''$ and $60''$, for NVSS, WENSS and GB6, respectively. This choice yields completeness of over 80% and a false matching rate below 1%.

The current positional overlap of the GB6, FIRST, NVSS, and WENSS catalogs includes 16,500 sources in about $3,000 \text{ deg}^2$. The matched sample is flux limited by GB6 for sources with spectral slope $\alpha < 0$, and by WENSS for sources with $\alpha > 0$, where $F_\nu \propto \nu^\alpha$. This is the largest database of the radio spectral and morphological measurements assembled to date.

For convenience, we express all fluxes on the AB_ν magnitude system of Oke & Gunn (1983), where $m = -2.5 \log(F_\nu/3631 \text{ Jy})$. The survey limits

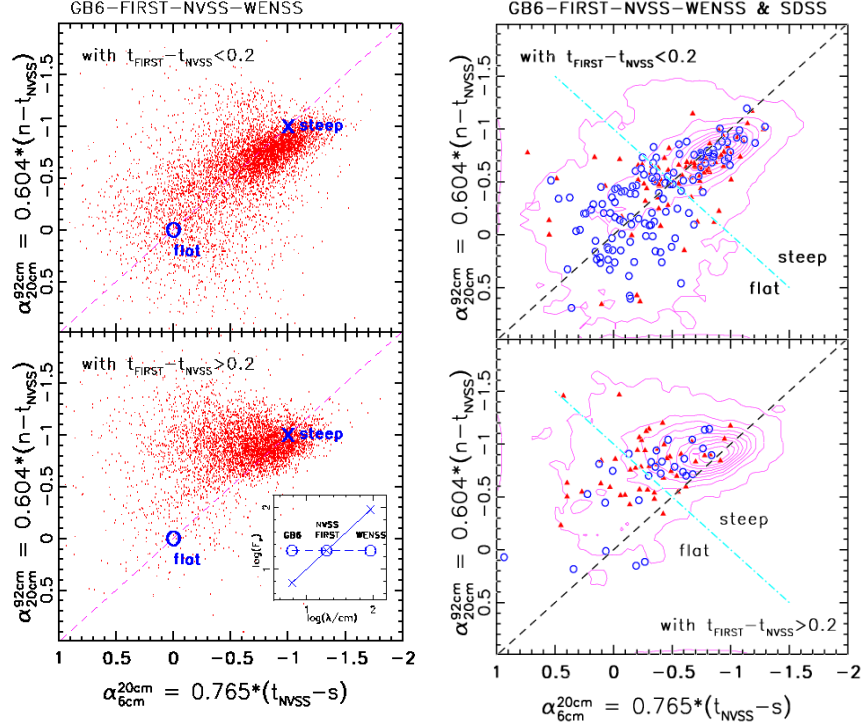


Figure 2. The distribution of radio sources detected by GB6, FIRST, NVSS, and WENSS in the 6-20-92 cm radio spectral slope diagram is shown in the two left panels for “core” (top) and “lobe” (bottom) sources, separated using the flux difference between FIRST and NVSS measurements. The diagonal dashed lines show the $y = x$ locus, with the positions for $\alpha = 0$ and $\alpha = -1$ marked as “flat” and “steep”, respectively. The SED difference between these two cases is illustrated in the insert in the bottom left panel. The two right panels compare the distributions of all matched radio sources (contours), to those for sources detected by the SDSS (triangles for galaxies and circles for quasars).

expressed in this system are $s < 13.3$, $t_{FIRST} < 16.4$, $t_{NVSS} < 15.4$, and $n < 13.3$, for GB6, FIRST, NVSS, and WENSS, respectively (magnitudes are named by the first letter of the corresponding wavelength in cm).

3. Radio Morphology from FIRST and NVSS Data

FIRST is a high resolution ($5''$) interferometric survey and thus over-resolves large sources relative to the lower resolution ($45''$) NVSS survey, leading to underestimated fluxes. Comparing the two surveys efficiently separates point and extended sources. The $\Delta t = t_{FIRST} - t_{NVSS}$ magnitude differences have a bimodal distribution (Figure 1) which reflects the separation between isolated core sources ($|\Delta t| < 0.2$) and lobe and com-

plex sources ($|\Delta t| > 0.2$). In addition to Δt , another useful morphological parameter is the ratio of integrated and peak FIRST fluxes – sources with $\theta = \log(F_{int}/F_{peak}) < 0.03$ appear unresolved by FIRST (Δt and θ are not equivalent because they measure size on different scales – $5''$ and $45''$).

4. Radio Color-Color Diagrams and Optical Identifications

The left panels in Figure 2 show the distributions of core (top) and lobe (bottom) sources (separated using $t_{FIRST} - t_{NVSS}$) in the 6-20-92 cm radio spectral slope (i.e. “color”-“color”) diagram. Note that there are more flat-spectrum sources in the top panel. According to size measurements from the FIRST survey and Figure 1, the overwhelming majority of flat-spectrum sources are also unresolved on $5''$ scales ($\theta < 0.03$) and on $45''$ scales. The right panels in Figure 2 compare the distributions of all matched radio sources (contours) to those for sources optically identified by SDSS. The compact flat-spectrum sources are dominated by quasars, while compact sources with steep spectra, and resolved radio sources, include substantial numbers of both quasars and galaxies. It is also noteworthy that the optically identified sources are *not* representative of the whole radio population.

5. Conclusions

The distribution of sources in radio “color-magnitude-morphology” space displays clear structure which encodes detailed information about the astrophysical processes that are responsible for the observed radio emission, and thus provides strong constraints for the models of these processes.

Acknowledgments

Funding for the creation & distribution of the SDSS Archive (<http://www.sdss.org/>) has been provided by the Alfred P. Sloan Foundation, the Participating Institutions, the National Aeronautics and Space Administration, the National Science Foundation, the U.S. Department of Energy, the Japanese Monbukagakusho, and the Max Planck Society.

References

1. Becker, R.H., White, R.L., & Helfand, D.J. 1995, ApJ, 450, 559
2. Condon, J. J., et al. 1998, AJ, 115, 1693
3. Gregory, P.C., et al. 1996, ApJS, 103, 427
4. Ivezić, Ž., et al. 2002, AJ, 124, 2364
5. Rengelink, R.B., et al. 1997, A&AS, 124, 259
6. Stoughton, C., et al. 2002, AJ, 123, 485
7. York, D.G., et al. 2000, AJ, 120, 1579